JPMTR 130 | 1914
DOI 10.14622/JPMTR-1914
UDC 651.5:546.57|7.048

Research paper
Received: 2019-12-25
Accepted: 2020-03-26

Optimisation of aerosol jet deposition for high-resolution selective patterning of silver tracks

Ben Clifford, Chris Phillips and Davide Deganello

Welsh Centre for Printing and Coating,
College of Engineering, Swansea University,
Fabian Way, Swansea, SA1 8EN, UK

b.r.clifford@swansea.ac.uk
c.o.phillips@swansea.ac.uk
d.deganello@swansea.ac.uk

Abstract

Aerosol jet deposition is a digital direct-write additive manufacturing technique capable of producing high resolution and highly customisable electronic and biological functional devices on both two- and three-dimensional substrates. This technology offers important market opportunities in the production of consumer electronics, semiconductor packaging, display technology, aerospace and defence, automotive and life sciences. However, for these opportunities to be realised there is a necessity for greater understanding of how deposition process parameters influence deposition quality. This study has explored the effects of a number of these parameters and their influence on the geometry of printed features. The results of this work outline the operating windows for several deposition parameters including carrier gas flow rate, stage speed working distance and stage temperature. Additionally, a number of relationships have been identified linking deposition parameters to the geometry of printed features.

Keywords: printed electronics, high-resolution printing, metal printing, parameter optimisation, surface topography

1. Introduction and background

Aerosol jet deposition is a direct-write non-contact deposition process originally developed for the manufacture of electronic circuits and printing of electronic materials. Since then its use as a deposition technology for a wide range of functional materials including metals, polymers and even biologicals has emerged (Zöllmer, et al., 2006). The compatibility of the technique with such a wide range of materials has seen the development of an assortment of novel applications in key research areas including printed electronics and sensors (Zhao, et al., 2012; Clifford, et al., 2018; Cantù, et al., 2018), renewable energy (Mette, et al., 2007) and biological/biomedical devices (Marquez, Renn and Miller, 2001).

Whilst the number of publications relating to aerosol jet deposition is increasing year on year, the majority of these are focussed on new applications of the technology and there is a lack of published research and understanding relating to the science and theory behind the process. This limited understanding in the field has resulted in recent publications reitterating the statement made over a decade ago that full and accurate process modelling and optimisation is required (Wilkinson, et al., 2019; Hon, Li and Hutchings, 2008; Zhang, Liu and Whalley, 2009).

The aerosol jet deposition process works by atomising, either ultrasonically or pneumatically, a solution or suspension containing a functional material suited to the desired application. Micron sized droplets become separated from the bulk material and become entrained in a carrier gas stream which transports them to a deposition head. This droplet loaded gas stream is then aerodynamically focussed by a secondary gas stream, referred to as the sheath gas, through a converging nozzle forming a collimated beam. The substrate is positioned several millimetres below the nozzle on a motion controlled heated stage, and patterning is achieved by the relative movement of the substrate and deposition head (Clifford, et al., 2018; Hoey, et al., 2012). A photograph of the aerosol jet deposition system at Swansea University with an illustrative diagram of the aerosol jet process is shown in Figure 1 (Clifford, 2017).

Process optimisation is complex with a large number of both primary and secondary parameters which can be varied to change the resolution and profile of depositions. On top of this, getting qualitative data from


a)

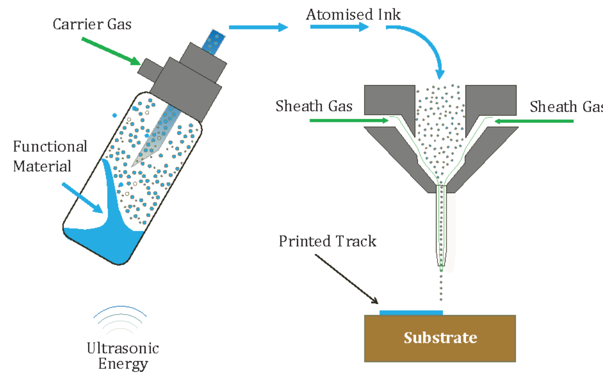

b)

Figure 1: (a) Photograph of the AJ300 aerosol jet deposition system at Swansea University; (b) an illustrative diagram showing the ultrasonic atomisation and aerosol jet deposition process

optical measurements of unoptimised prints is often complicated by poorly defined edges and unwanted deposition phenomena including overspray and satellite droplets.

In 2011, Goth, Putzo and Franke described the main influencers affecting aerosol jet deposition quality, grouping them into six categories: robot, process control, operator, ink, substrate and environment, each containing a set of individual parameters. An adapted Ishikawa diagram based on the work presented by Goth, Putzo and Franke (2011) is shown in Figure 2 highlighting these categories.

Whilst there are several research papers looking at parametric studies of the aerosol jet system, the majority of the work is directed to exploring the influence of the ratio of the carrier gas and sheath gas flow rates (Mahajan, Frisbie and Francis, 2013; Arsenov, Efimov and Ivanov, 2018). In this paper, we present a study of the effects of several additional process parameters, namely, atomiser (or carrier) gas flow rate; working (nozzle-substrate) distance; stage speed and stage temperature, on the geometry of printed silver lines.

The findings of this work can be used to identify the operating window of individual parameters as well to outline those that are critical to achieving high-resolution features as well as secondary and complementary parameters.

2. Materials and methods

2.1 Ink

All printing during the process study was carried out using a commercial nanoparticle silver ink TPS 35 HE (Clariant Produkte (Deutschland) GmbH). This ink is designed to be used for inkjet printing and is quoted as having a dynamic viscosity of 6.5 mPas at 20 °C and a surface tension of 28.2 mN/m. The solids loading of this ink is approximately a mass fraction of 35 % with an average particle size of approximately 60 nm. The solvent in which the particles are dispersed is a blend of water and ethylene glycol. In order to make this ink compatible with the ultrasonic atomiser of the aerosol jet system, it was diluted with distilled water at a ratio of 1:2 parts by volume.

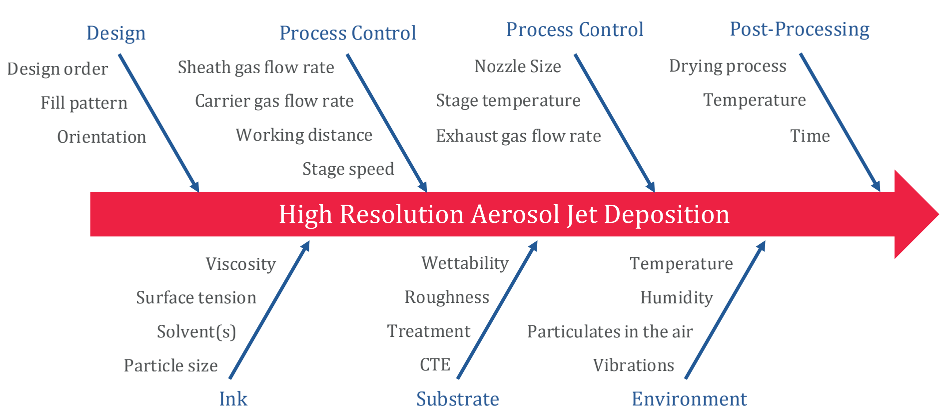

Figure 2: An Ishikawa diagram showing the large parameter set affecting aerosol jet deposition feature geometry and resolution

2.2 Substrate

Standard glass microscope slides (12383118, Fisher Scientific) of length and width of 76 mm and 26 mm with a thickness between 1 and 1.2 mm were used as the test substrate. Glass microscope slides were chosen for their low roughness, transparency and consistency between batches. The low roughness provided a clean base for surface topology and profile measurements whilst the transparency allowed backlit illumination to be used in the detection of overspray. The average surface roughness, S_a, and the root mean square (RMS) surface roughness, S_q, of these microscope slides was measured using white light interferometry to be 9.18 nm and 12.73 nm, respectively.

Prior to deposition, the glass slides were prepared by ultrasonic cleaning in acetone, propan-2-ol and deionised water for 10 minutes in each. Following the cleaning process the glass slides were dried and placed on a hot plate at 200 °C for 30 minutes before they were transferred to the system for printing. The deposited ink showed good levels of wetting with the cleaned glass slides and hence no additional surface pre-treatment/modification was required.

2.3 Printing methodology

Deposition was performed with an AJ300 aerosol jet deposition system (Optomec Inc., Albuquerque, USA) using an ultrasonic atomiser operating at 2.4 MHz. For all experiments a number of parameters including the nozzle, atomiser power and ink temperature were kept constant. The nozzle used had a 200 μm diameter opening with a taper half angle of a few degrees. The atomiser power was set to ≈ 31 W by applying a voltage of 48 V and a current of ≈ 650 mA. For each print run, the atomiser vial was loaded with 1.80 ml of the diluted ink described in section 2.1 and maintained at 20 °C by means of a temperature-controlled water bath.

Two designs were selected as test patterns to allow geometric characterisation in terms of line width and height whilst providing the ability to identify the effects of varying these parameters on overspray and satellite deposition. The first toolpath consisted of six parallel horizontal lines each positioned 1 mm apart; three lines of 10 mm in length and three lines of 20 mm in length to allow testing at high (≥ 10 mm/sec) process velocities whilst ignoring any initial acceleration. The second design was a smaller serpentine pattern of length 5 mm and pitch of 0.5 mm used to create prints which could be optically imaged in a single scan.

Following deposition, samples were dried in a natural convection oven (UNB400, Memmert GmbH) at 200 °C for 60 minutes and stored in sealed Petri dishes prior to measurement and analysis.

Prior to performing the experiments described, a literature survey and initial screening trial was performed to identify suitable parameters and the operating ranges for each. This revealed a number of parameters that have a significant impact on deposition quality. The work presented here shows the results of adjusting these key parameters and full results including secondary parameters can be seen in the thesis titled "Optimisation of Aerosol Jet Deposition for the Development of Printed Electronics" (Clifford, 2017).

The parameters studied in this work are shown in Table 1 along with the ranges used for testing. For each parameter investigated three prints were produced, with 30 measurements made across each sample (5 equidistant points on each line) giving a total of 150 data points per variation.

The carrier gas flow rate determines the quantity of atomised material that is transferred to the deposition head and one of two parameters affecting the volume of material deposited in one location on the substrate. The stage speed is the second of these parameters and controls the process velocity of the stage, and substrate, relative to the deposition head. The carrier gas flow rate and stage speed have a positive relationship meaning as the atomiser flow rate is increased the stage speed must also be increased to produce the same geometry features. As material exits the nozzle as a highly collimated stream the sheath gas immediately begins to diverge giving the stream a limited

Table 1: The parameters tested with a brief description of what they affect with the range of values that were tested

Parameter	Description	Range Tested
Carrier Gas Flow Rate	Controls the quantity of material delivered to the deposition head.	12–24 cm^3/min
Stage Speed	The speed the stage (and substrate) moves relative to the fixed deposition head and nozzle.	1–10 mm/sec
Nozzle–Substrate Distance	The distance material travels between exiting the nozzle and impacting with the substrate.	2–11 mm
Stage Temperature	The temperature of the stage that the substrate is positioned on during printing.	25–100 °C

focussing length. The distance between the nozzle exit and the substrate whereby the material stream needs to remain focussed is termed the nozzle–substrate distance. The stage temperature affects the drying rate of the deposited material and as such the final geometry of printed features.

2.4 Surface topography measurement

Optical images of deposited features were gathered using an Alicona G5 infinite focus microscope (Alicona Imaging GmbH, Austria) in order to visually explore deposition quality. As well as visualisation of the deposits, this provided a method to qualitatively assess the deposited features in terms of unwanted attributes such as overspray and satellite deposition.

White light interferometry (NT9300, Veeco Instruments Inc., Plainview, NY, USA) was used to obtain surface topography data for each printed line. Measurements were collected at eleven times magnification (achieved using a twenty times magnification lens with a 0.55 times field of view modifier), giving a measurement area of 0.58 mm by 0.43 mm at a resolution of 640 × 480 pixels. For each print, the geometry was measured at ten discrete points along the length of the line. Measurements were taken of the line width and average height (taken as the average height of the substrate subtracted from the average height of the ink) as well as reviewing the profile shape.

3. Results and discussion

3.1 Carrier gas

The carrier gas flow rate is one of two primary parameters affecting the volume of material deposited in one location – the other being the stage speed. In order to investigate the effect of the carrier gas flow rate on the geometry of printed features, deposition was performed at a range of carrier gas flow rates between 12 cm^3/min and 24 cm^3/min whilst maintaining a constant sheath gas flow rate of 90 cm^3/min. Additionally, the stage speed was maintained at a constant value of 1 mm/s with a stage temperature of 100 °C.

The measured line width and average line height data is plotted graphically in Figures 3a and 3b separately.

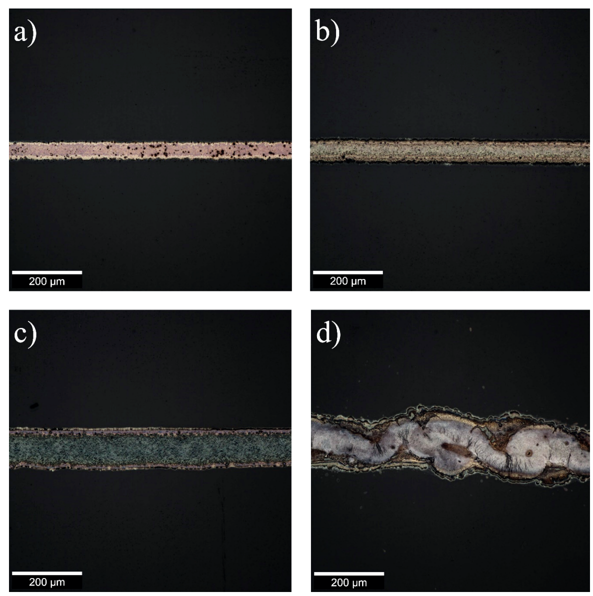

Figure 4: Optical microscope images showing the effect of carrier gas flow rate of (a) 12 cm^3/min, (b) 16 cm^3/min, (c) 20 cm^3/min, and (d) 24 cm^3/min on deposited line geometry using a constant sheath gas flow rate of 90 cm^3/min; scale bar for reference is 200 µm

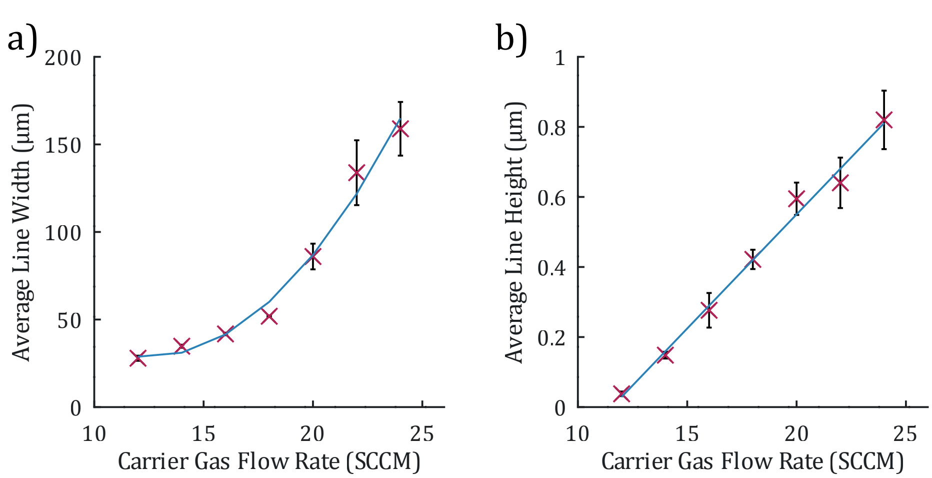

Figure 3: Graphs showing the effect of carrier gas flow rate on (a) average line width, and (b) average line height

The data shows that as the carrier gas flow rate increases both the width and height of deposited line also increases. Initially, for carrier gas flow rates between 12 cm^3/min and 18 cm^3/min the line width shows a linear trend with low standard deviations but as the flow rate increases further the line width and standard deviation increase rapidly diverging from the trend. This sudden increase is linked to the stage speed being too low allowing large quantities of material to build up in one location. This can be seen visually in the optical microscope images shown in Figures 4a to 4d taken of lines deposited at carrier gas flow rates of 12 cm^3/min, 16 cm^3/min, 20 cm^3/min and 24 cm^3/min, respectively.

3.2 Stage speed

The stage speed is the second parameter affecting the volume of material deposited in one location. In order to investigate the effect of stage speed on the geometry of printed features (Figure 5), deposition was performed at stage speeds between 1 mm/s and 10 mm/s. During the experiment, the sheath and carrier gas flow rates were kept constant at 112 cm^3/min and 16 cm^3/min, respectively. The stage temperature was maintained at a constant value of 100 °C.

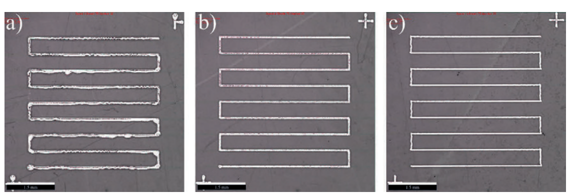

Figure 5: Optical microscope images showing the effect of stage speed on deposited line geometry; stage speed of (a) 1 mm/s, (b) 4 mm/s, and (c) 10 mm/s; scale bar for reference is 1.5 mm

The average line width and line height data are plotted graphically in Figures 6a and 6b separately. From these graphs it can be seen that as the stage speed increases there is a decrease in both line width and line height as less material is deposited in each area. The line width and height decrease steadily as stage speed increases from 1 mm/s to 3 mm/s. After this point, the sensitivity of the deposit to stage speed is reduced. The rate of decrease in line width and height is higher at low speed transitions due to the larger printed length for the given carrier gas flow rate. As an example, with the sheath and carrier gas flow rates described previously, an increase in stage speed from 1 mm/s to 2 mm/s causes a decrease in line width of 11.22 µm. In contrast at the same flow rates, an increase in stage speed from 6 mm/s to 7 mm/s causes a much smaller drop in line width – 1.29 µm. This highlights the relationship between the carrier gas flow rate and the stage speed previously discussed.

3.3 Nozzle–substrate distance

As a result of the nozzle profile and annular sheath gas flow, the material exits the nozzle as a highly collimated converging beam which becomes finest at a focal point before rapidly diverging. In order to investigate the effect of the nozzle-substrate distance on the geometry of printed features, deposition was performed with the nozzle positioned between 2 mm and 11 mm above the substrate. During the experiment, both the carrier and sheath gas flow rates were kept constant at 20 cm^3/min and 100 cm^3/min, respectively. The stage speed was set to 2 mm/s with the temperature at 100 °C.

At each working distance, measurements of line width and height were taken using white light interferometry as well as imaged using optical microscopy. For each printed line multiple measurements were performed using white light interferometry, and the results are presented graphically in Figure 7. Due to the poor quality and large amounts of overspray and satellite deposition seen in the lines deposited at working distances greater than 9 mm it was not possible to obtain line width and line height measurements.

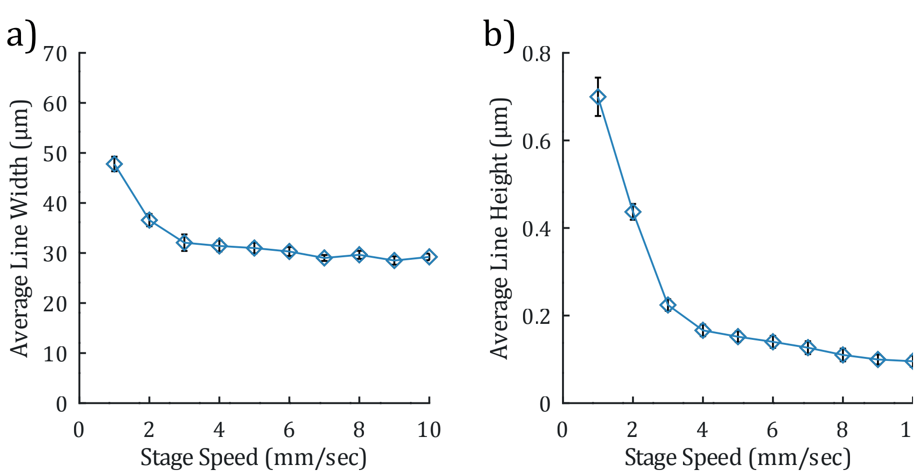

Figure 6: Graphs showing the effect of stage speed on (a) average line width, and (b) average line height

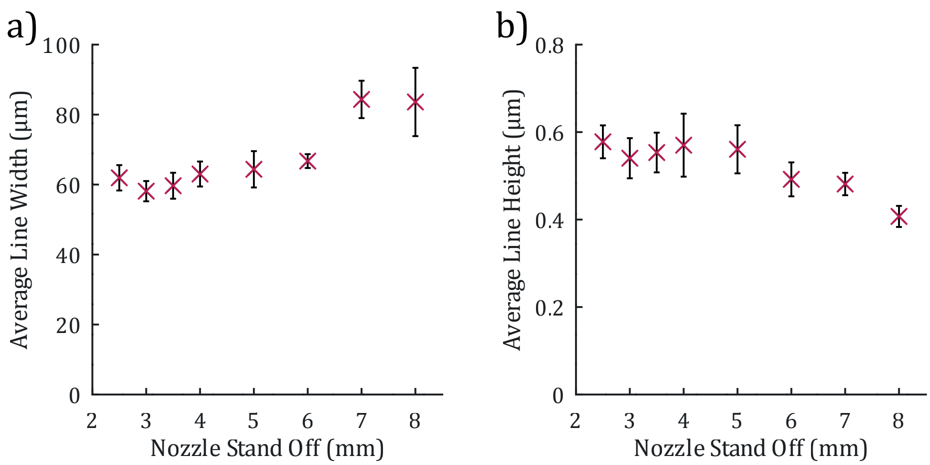

Figure 7: Graphs showing the effect of nozzle–substrate distance on (a) average line width, and (b) average line height

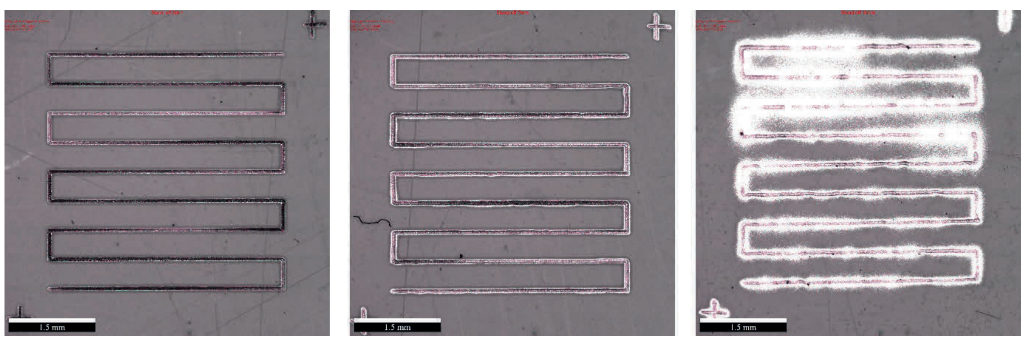

Figure 8: Optical microscope images showing the effect of nozzle–substrate distance on deposited line geometry; on deposited line with a nozzle–substrate distance of (a) 3 mm, (b) 7 mm, and (c) 11 mm; scale bar for reference is 1.5 mm

Figure 8 shows microscope images of a low-density serpentine pattern deposited at nozzle–substrate distances of 3 mm (Figure 8a), 7 mm (Figure 8b) and 11 mm (Figure 8c). The line deposited at a working distance of 3 mm has well defined edges with no visible overspray, the line deposited at a working distance of 7 mm has some observable waviness at the edges with small amounts of overspray. In contrast the line deposited at a working distance of 11 mm has poorly-defined edges with large amounts of overspray obscuring the printed pattern.

3.4 Stage temperature

During deposition the substrate is positioned on a heated stage to aid in the drying of the ink. In order to investigate this parameter, the carrier and sheath gas flow rates were kept constant at 18 cm^3/min and 72 cm^3/min respectively with the stage speed set to 3 mm/s. The stage temperature was varied between 25 °C and 100 °C in increments of 25 °C with the purpose of investigating its effect on the deposited line geometry.

For each printed line multiple measurements were performed using white light interferometry and the results are presented graphically in Figure 9.

Figure 9 shows the effect of increasing stage temperature on line geometry. For stage temperatures below 100 °C, as the temperature increases the width of line also increases. In contrast, at a stage temperature of 100 °C a decrease in the line width is observed.

Additionally, as the stage temperature increases the standard deviation in the average line width decreases from 1.99 μm at 25 °C to 1.32 μm at 100 °C. Since the ink contains a volume fraction of approximately 84 % water which has a boiling point of around 100 °C, a large percentage of the water content is readily evaporated upon impact with the substrate. This could explain the decreased average line width at a stage temperature of 100 °C but further investigation is required involving inks containing different boiling point solvents. This explanation is also supported by examining the profiles of deposited lines at each stage temperature as shown in Figure 10.

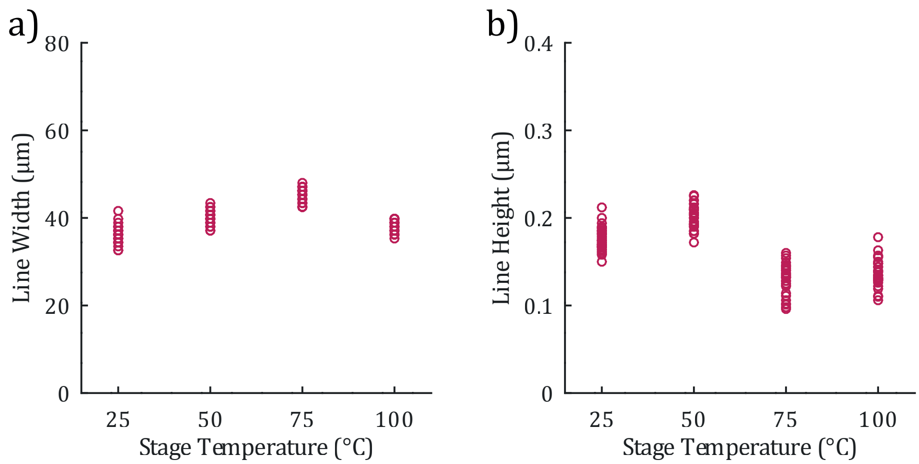

Figure 9: Graphs showing the effect of stage temperature on (a) average line width, and (b) average line height

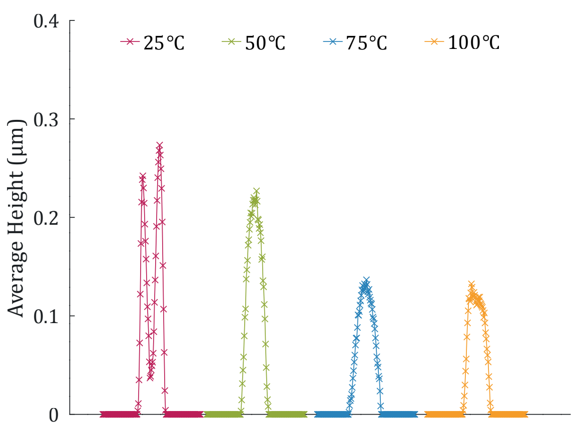

Figure 10: A graph showing the effect of stage temperature on the profile shape of deposited lines

By studying the visualisation in Figure 10, significant differences can be seen between the line profiles as a result of different stage temperatures.

At 25 °C the profile shows two distinct peaks with a central void often described in printing terminology as coffee-stain effect. As the stage temperature increases the height of the line profile reduces and the profile becomes more rectangular at 100 °C.

3.5 Deposition quality achieved with the optimised parameters

The optimisation of the parameters discussed has allowed for deposition of high resolution printed features as shown in Figures 11 and 12.

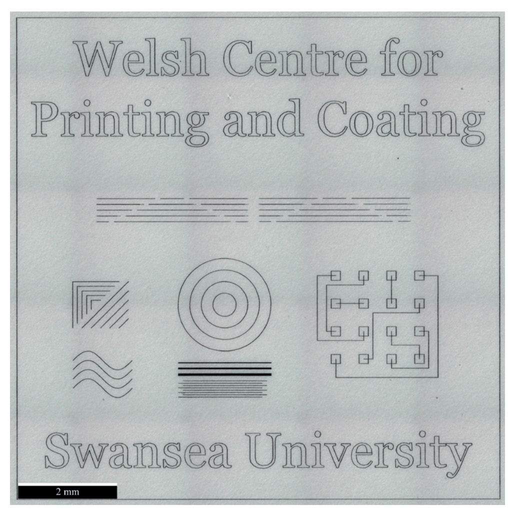

Figure 11: A microscope image showing a test pattern printed using aerosol jet deposition; scale bar for reference is 2 mm

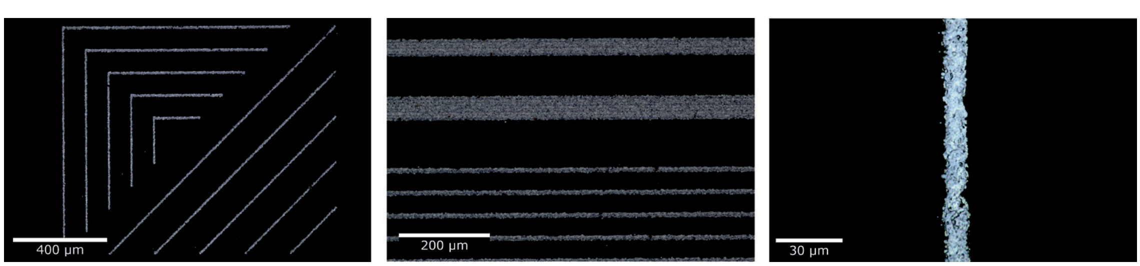

a) b) c)

Figure 12: Microscope images showing close up images of the features in Figure 11; scale bars are on (a) 400 µm, (b) 200 µm, and, (c) 30 µm, respectively (note: The contrast of this image has been adjusted in GIMP 2.10.14)

The deposited features have an average line width of around 10 μm with low amounts of overspray and satellite deposition with other lines shown with line widths of 30 μm, 40 μm and 50 μm.

4. Conclusions

From this study, the stage temperature and nozzle–substrate distance have been identified as critical parameters to obtaining high resolution defect free deposition. The stage temperature has been shown to have a significant effect on the geometry and resolution of printed features which has been theorised to be as a result of the formulation of the ink being tested. A relationship has been identified between the nozzle–substrate distance and unwanted deposition phenomena such as overspray and satellite droplets affecting overall resolution.

The effects of varying the carrier gas flow rate and stage speed have been shown to be linked to one another and whilst they do affect the geometry of deposited features, they do not directly affect resolution within their normal operating ranges. It is also possible to adjust these parameters in parallel to allow for thicker deposits with larger volumes of material or to maintain thinner deposits but reduce overall print time.

Whilst a significant number of parameters have been evaluated in this work, there are still parameters which have not been reviewed as well as other relationships that may be exist with relation to print design and material formulation.

Acknowledgements

This work was financially supported by the College of Engineering at Swansea University. The authors would also like to acknowledge the Centre for NanoHealth (CNH) at Swansea University for access to facilities and equipment.

References

Arsenov, P.V., Efimov, A.A. and Ivanov, V.V., 2018. Effect of methods of changing in focusing ratio on line geometry in aerosol jet printing. Key *Engineering Materials*, 779, pp. 159–164. https://doi.org/10.4028/www.scientific.net/KEM.779.159.

Cantù, E., Tonello, S., Abate, G., Uberti, D., Sardini, E. and Serpelloni, M., 2018. Aerosol jet printed 3D electrochemical sensors for protein detection. *Sensors,* 18(11): 3719. https://doi.org/10.3390/s18113719.

Clifford, B., 2017. *Optimisation of aerosol jet deposition for the development of printed electronics*. Ph.D. thesis. Swansea University.

Clifford, B., Beynon, D., Phillips, C. and Deganello, D., 2018. Printed-sensor-on-chip devices – aerosol jet deposition of thin film relative humidity sensors onto packaged integrated circuits. *Sensors and Actuators B: Chemical*, 255(1), pp. 1031–1038. https://doi.org/10.1016/j.snb.2017.08.086.

Goth, C., Putzo, S. and Franke, J.K.H., 2011. Aerosol jet printing on rapid prototyping materials for fine pitch electronic applications. In: *IEEE 61st Electronic Components and Technology Conference (ECTC)*. Lake Buena Vista, FL, USA, 31 May–3 June 2011. IEEE. https://doi.org/10.1109/ECTC.2011.5898664.

Hoey, J.M., Lutfurakhmanov, A., Schulz, D.L. and Akhatov, I.S., 2012. A review on aerosol-based direct-write and its applications for microelectronics. *Journal of Nanotechnology*, 2012: 324380. https://doi.org/10.1155/2012/324380.

Hon, K.K.B., Li, L. and Hutchings, I.M., 2008. Direct writing technology – advances and developments. *CIRP Annals – Manufacturing Technology*, 57(2), pp. 601–620. https://doi.org/10.1016/j.cirp.2008.09.006.

Mahajan, A., Frisbie, C.D. and Francis, L.F., 2013. Optimization of aerosol jet printing for high-resolution, high-aspect ratio silver lines. *ACS Applied Material & Interfaces*, 5(11), pp. 4856–4864. https://doi.org/10.1021/am400606y.

Marquez, G.J., Renn, M.J. and Miller, W.D., 2001. Aerosol-based direct-write of biological materials for biomedical applications. *MRS Online Proceedings Library*, 698: Q5.2.1. https://doi.org/10.1557/PROC-698-Q5.2.1.

Mette, A., Richter, P.L., Hörteis, M. and Glunz, S.W., 2007. Metal aerosol jet printing for solar cell metallization. *Progress in Photovoltaics: Research and Applications*, 15(7), pp. 621–627. https://doi.org/10.1002/pip.759.

Wilkinson, N.J., Smith, M.A.A., Kay, R.W. and Harris, R.A., 2019. A review of aerosol jet printing — a non-traditional hybrid process for micro-manufacturing. *The International Journal of Advanced Manufacturing Technology*, 105, pp. 4599–4619. https://doi.org/10.1007/s00170-019-03438-2.

Zhang, Y., Liu, C. and Whalley, D.C., 2009. Direct-write techniques for maskless production of microelectronics: a review of current state-of-the-art technologies. In: *International Conference on Electronic Packaging Technology & High Density Packaging (ICEPT-HDP '09)*. Beijing, China, 10–13 August 2009. IEEE, pp. 487–503. http://dx.doi.org/10.1109/ICEPT.2009.5270702.

Zhao, D., Liu, T., Zhang, M., Liang, R. and Wang, B., 2012. Fabrication and characterization of aerosol-jet printed strain sensors for multifunctional composite structures. *Smart Materials and Structures*, 21(11): 115008. https://doi.org/10.1088/0964-1726/21/11/115008.

Zöllmer, V., Müller, M., Renn, M., Busse, M., Wirth, I., Godlinski, D. and Kardos, M., 2006. Printing with aerosols: a maskless deposition technique allows high definition printing of a variety of functional materials. *European Coatings Journal*, 07–08: 46.